Dosimetric accuracy of three dose calculation algorithms for radiation therapy of in situ non- small cell lung carcinoma

Švabić Kolacio, Manda; Rajlić, David; Radojčić, Milan; Smilović Radojčić, Đeni; Obajdin, Nevena; Dundara Debeljuh, Dea; Jurković, Slaven

Source / Izvornik: **Reports of Practical Oncology and Radiotherapy, 2022, 27, 86 - 96**

Journal article, Published version
Rad u časopisu, Objavljena verzija rada (izdavačev PDF)

https://doi.org/10.5603/RPOR.a2022.0013

Permanent link / Trajna poveznica: https://urn.nsk.hr/urn:nbn:hr:184:442554

e-ISSN 2083–4640
ISSN 1507–1367

RESEARCH PAPER

Reports of Practical Oncology and Radiotherapy
2022, Volume 27, Number 1, pages: 86–96
DOI: 10.5603/RPOR.a2022.0013
Submitted: 09.11.2021
Accepted: 19.01.2022

Dosimetric accuracy of three dose calculation algorithms for radiation therapy of in situ non-small cell lung carcinoma

Manda Švabić Kolacio[1], David Rajlić[1], Milan Radojčić[2], Đeni Smilović Radojčić[1, 3], Nevena Obajdin[1], Dea Dundara Debeljuh[1, 3, 4], Slaven Jurković[1, 3]

[1]Medical Physics Department, Clinical Hospital Center Rijeka, Rijeka, Croatia
[2]Clinic for Radiotherapy and Oncology, Clinical Hospital Center Rijeka, Rijeka, Croatia
[3]Department of Medical Physics and Biophysics, University of Rijeka Faculty of Medicine, Rijeka, Croatia
[4]Radiology Department, General Hospital Pula, Pula, Croatia

ABSTRACT

Background: Study determines differences in calculated dose distributions for non-small cell lung carcinoma (NSCLC) patients. NSCLC cases were investigated, being the most common lung cancer treated by radiotherapy in our clinical practice.

Materials and methods: A retrospective study of 15 NSCLC patient dose distributions originally calculated using standard superposition (SS) and recalculated using collapsed cone (CC) and Monte Carlo (MC) based algorithm expressed as dose to medium in medium (MCD_m) and dose to water in medium (MCD_w) was performed so that prescribed dose covers at least 99% of the gross target volume (GTV). Statistical analysis was performed for differences of conformity index (CI), heterogeneity index (HI), gradient index (GI), dose delivered to 2% of the volume ($D_{2\%}$), mean dose (D_{mean}) and percentage of volumes covered by prescribed dose (V_{70Gy}). For organs at risk (OARs), D_{mean} and percentage of volume receiving 20 Gy and 5Gy (V_{20Gy}, V_{5Gy}) were analysed.

Results: Statistically significant difference for GTVs was observed between MCD_w and SS algorithm in mean dose only. For planning target volumes (PTVs), statistically significant differences were observed in prescribed dose coverage for CC, MCD_m and MCD_w. The differences in mean CI value for the CC algorithm and mean HI value for MCD_m and MCD_w were statistically significant. There is a statistically significant difference in the number of MUs for MCD_m and MCD_w compared to SS.

Conclusion: All investigated algorithms succeed in managing the restrictive conditions of the clinical goals. This study shows the drawbacks of the CC algorithm compared to other algorithms used.

Key words: radiation therapy; TPS; non-small cell lung carcinoma; Monaco; XiO standard superposition

Rep Pract Oncol Radiother 2022;27(1):86–96

Introduction

Accuracy of dose calculation algorithms is one of the prerequisites for successful radiation therapy outcome. Thorough investigation of possible limitations of calculation algorithms is important because the total error in delivered absorbed dose of 5% can lead up to at least 20% of change in Tumour Control Probability (TCP) and Normal Tissue Complication Probability (NTCP) [1, 2]. Therefore, the quantification and characterization of possible sources of errors in absorbed dose calculation is required.

Address for correspondence: Slaven Jurković, Krešimirova 42; 51 000 Rijeka; Croatia, tel:+385 51 658 599; e-mail: slaven.jurkovic@medri.uniri.hr

The introduction of a more advanced Elekta Monaco treatment planning system (TPS) at the Radiation Oncology Department of the University Hospital Rijeka opened the possibility of optimisation and calculation of absorbed dose distributions for the planning of certain tumour sites using different dose calculation algorithms. Until recently, the radiation therapy planning technique of choice for Non-Small Cell Lung Carcinoma (NSCLC) was forward planned intensity modulated radiation therapy (IMRT) using the standard superposition (SS) analytical dose calculation algorithm built in the Elekta XiO TPS. After commissioning and clinical implementation of the Elekta Monaco TPS, the intention was to transfer the workflow for NSCLC cases to the advanced TPS. Elekta Monaco TPS uses the collapsed cone (CC) analytical dose calculation algorithm for forward planning IMRT and a Monte Carlo (MC) based algorithm for inverse planning IMRT.

The clinical impact of using different dose calculation algorithms, especially comparisons taking into account MC based algorithms, have been in focus of research since their implementation in radiation oncology and are still an interesting research topic [3–9]. Considering the known differences in dose calculation engines of the abovementioned algorithms, especially in low-density media, it was decided to investigate lung cancer patients, specifically NSCLC cases, because they are the most common in our clinical practice.

Prior to implementation of SS algorithm into clinical practice, a thorough validation of absorbed dose calculation accuracy of the algorithm compared to measurements in the CIRS Thorax semi-anthropomorphic phantom was performed [10]. In order to investigate the dosimetric accuracy of absorbed dose calculation of the algorithms built in the Elekta Monaco TPS, the same set of calculations and measurements was repeated [11, 12]. Discrepancies between measured and calculated dose in lung density equivalent (LDE) and bone density equivalent (BDE) regions of the phantom were observed for the algorithms built in the Elekta Monaco TPS. For the MC based Monaco algorithm, similar behaviour in BDE was reported in earlier studies [13, 14]. Magnitude of reported discrepancies could be related to the dose calculation algorithm used. Considering that, observed discrepancies in the LDE regions raise the question of possible clinical implications for lung cancer patients. Thus, the dosimetric evaluation results in semi-anthropomorphic phantom incited the main focus of this paper to be an investigation of possible clinical impact. Consequently, the evaluation of performance and possible limitations of algorithms built in Monaco TPSs for patients with in-situ NSCLC, considering the large regions of low-density tissue encompassed in irradiated volumes, was examined.

Materials and methods

Treatment planning

This work was performed using devices which are in clinical use at the Radiation Oncology Department of University Hospital Rijeka: linear accelerator Siemens Oncor Expression, Siemens Somatom Open CT simulator (Siemens Healthineers, Erlangen, Germany) and TPSs XiO v.5.10.02 and Monaco v.5.11.02 (Elekta, Stockholm, Sweden).

The intention of research was not a thorough examination of algorithm performances but the verification of acceptability of calculated absorbed dose for NSCLC patients. Nevertheless, it is necessary to emphasize the basic differences within dose calculation engines built in algorithms used in this study. Namely, the Elekta XiO SS analytical algorithm utilizes the patient CT data as water with variable electron densities for absorbed dose calculation and, consequently, expresses dose as dose to water in water [15]. In the Elekta Monaco CC analytical algorithm the dose concept is to calculate the dose to actual medium and, therefore, report dose to medium [16, 17]. The absorbed dose calculation algorithm built in the Elekta Monaco TPS used for inverse IMRT planning is based on MC simulation (X-ray Voxel Monte Carlo, XVMC) in a patient model [18]. It provides two dose reporting modes: dose to medium in medium (MCD_m) and dose to water in medium (MCD_w). For the MC based algorithm, there is neither general agreement [13, 19–21] nor recommendation which reporting mode should be used for expressing dose in clinical cases. Thus, absorbed dose distributions created for this retrospective study were calculated and optimized using both approaches. Statistical uncertainty (SU) used for both dose calculations was 0.5% per control point. It is worth noting that the results of the investigation of our group using *ab initio* MC simulation for the absorbed dose calcula-

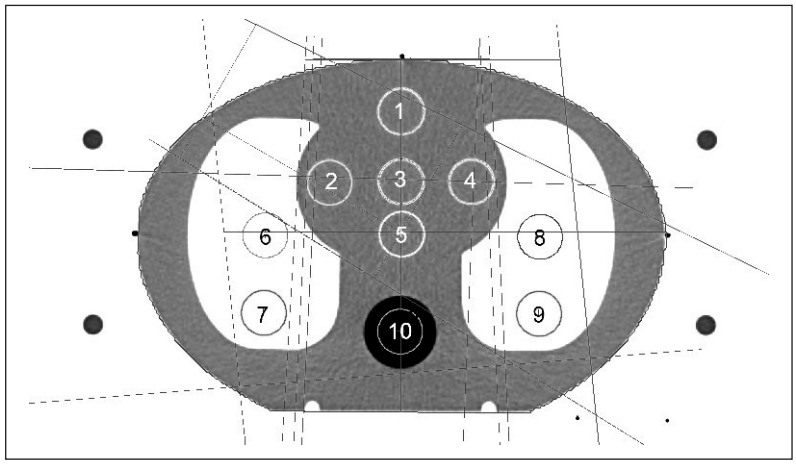

Figure 1. Cross section of CIRS Thorax phantom with three regions of different densities: water density equivalent (WDE) region (plastic water, ρ = 1.003 g/cm^3) with measuring points 1–5, lung density equivalent (LDE) region (ρ = 0.207 g/cm^3) with measuring points 6–9 and bone density equivalent (BDE) region (ρ = 1.506 g/cm^3) with measuring point 10

tion in low-density media and simple geometries show that the MCD_m and MCD_w reporting modes can be considered equivalent [22]. Further work will be dedicated to verify the aforementioned results in clinical cases.

Phantom measurements

The dosimetric accuracy of investigated algorithms for 6MV photon beam was initially verified through absorbed dose measurements in a water phantom. TPS dose point values were used for the analytical algorithms used in this study. For both calculation options of the MC algorithm, the dose calculation was averaged over a 0.081 cm^3 spherical volume with 81 dose evaluation points. Discrepancies for examined algorithms between measured and calculated data in water were determined according to international recommendations [11, 12, 23]. Evaluation of the results was performed using the expression:

$$\Delta[\%] = 100 \bullet \left(\frac{D_{calc} - D_{meas}}{D_{meas,ref}} \right) \quad (1)$$

where,

D_{calc} is calculated dose at a particular point in the phantom, D_{meas} is the measured dose at the point of calculation in the phantom, $D_{meas,ref}$ is the measured dose at the reference point in the phantom.

The algorithms were further validated using the semi-anthropomorphic CIRS Thorax phantom, made from three different density regions (water density equivalent — WDE, LDE and BDE) (Fig. 1). The phantom was scanned using the standard CT protocol for lung cancer patients (120 kVp tube voltage, 95 mAs, 3 mm slice thickness, extended field of view), contoured and used for dose calculations. Measurements were performed at 10 points in the phantom using the PTW30013 ionization chamber.

Absorbed dose calculations provided by above mentioned algorithms were verified in a semi-anthropomorphic phantom for different beam arrangements following the recommendations [11, 12]. Discrepancies were calculated using Eq. 1. Tolerances were determined considering the complexity of the measurement geometry [24]. Furthermore, the results with large measurement uncertainty (areas of large dose gradient and radiation fields smaller than 4 × 4 cm^2) were excluded from the analyses. For points located in the WDE region of the phantom, the tolerances were up to ± 3%, while in the non-water equivalent regions, the tolerance limits were up to ± 4%. One has to bear in mind that dosimetric validation has its own intrinsic limitations depending on the uncertainties of the dosimetrical system used, especially for measurements in non-water density equivalent media [25].

Clinical study design

To investigate possible implications of used calculation algorithms on radiation therapy treatment, a retrospective study of 15 NSCLC patients was performed. Dose distributions for these pa-

tients were originally calculated using the SS algorithm. For the purpose of this study, the absorbed dose distributions were created again using the Elekta Monaco inverse and forward planning IMRT modes by applying the MC based and CC algorithms, respectively. Beam angles and target margins were maintained in order to avoid variability in the results due to different beam arrangements. The patients underwent CT simulation in a supine position with free breathing conditions using standard lung cancer patient CT acquisition protocol. Conventional fractionation of 2 Gy per fraction was prescribed while the total dose was patient dependent. It was determined by the radiation oncologist considering patient age, general condition, comorbidities and lungs functional status (FEV1-forced expiratory volume in the first second and DLCO-diffusing capacity of the lungs for carbon monoxide). GTV was defined as a visible tumour along with enlarged lymph nodes with short axis diameter larger than 10 mm. The PTV margin for non-central lesions was 8–10 mm, except in the craniocaudal direction for which it was 10–15 mm depending on the tumour location [26–28]. GTV volumes ranged from 28.37 to 130.05 cm^3 and PTV volumes varied between 95.3 and 366.3 cm^3. All patients had solid tissue equivalent density GTVs. These patients were selected for their relatively small GTV volumes compared to their corresponding PTV volumes and large V_{PTV}/V_{GTV} ratios with PTVs including a high amount of lung tissue. In Figure 2 typical transversal CT slice of a patient included in the study is shown. Large difference in PTV and GTV volumes is noticeable.

Planning objectives regarding the target volumes (TVs) and relevant organs at risk (OARs) were achieved in accordance with international guidelines [27, 29]. All dose distributions were calculated and optimized in a way that at least 99% of the GTV should be covered by the prescribed dose. The dose calculation voxel size was $3 \times 3 \times 3$ mm^3 for all calculations. For inverse IMRT the minimum open field size was 4 cm^2, the statistical uncertainty was kept at 0.5% per control point and the minimum number of monitor units (MUs) per segment was 2. The IMRT delivery mode was step and shoot. To facilitate intercomparation regardless of the original patient dose prescription, all absorbed dose distributions were set to 70 Gy (2 Gy per fraction, 35 fractions).

Statistical analysis

Calculated dose volume histograms (DVH) were analysed to quantify the dose to TVs and relevant OARs. Maximum dose defined as dose delivered to 2% of the volume ($D_{2\%}$), mean dose (D_{mean}) and percentage of volumes covered by the prescribed dose were also used to validate dose distribution differences for planning target volumes (PTVs) and gross tumour volumes (GTVs). For the OARs (ipsilateral, contralateral and whole lungs), D_{mean} and percentage of volume receiving 20 Gy and 5 Gy (V_{20Gy}, V_{5Gy}), were validated [30–32].

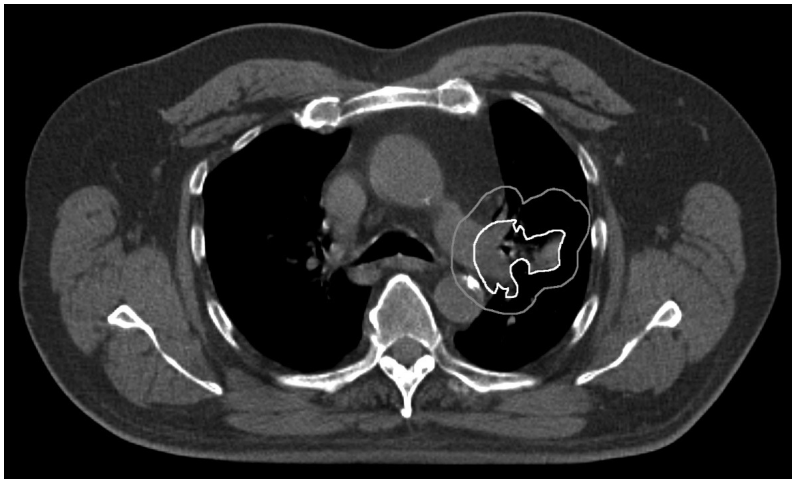

Figure 2. Example of typical transversal CT slice of a patient included in the study showing large difference in the planning target volume (PTV) (grey line) and the gross target volume (GTV) (white line) volume as well as large lung volume included in the PTV

Additional analysed parameters were: heterogeneity index (HI) (Eq. 2), conformity index (CI) (Eq. 3) and gradient index (GI) (Eq. 4) defined as:

$$HI = \frac{D_{2\%}}{D_{98\%}} \quad (2)$$

$$CI = \frac{TV_1^2}{TV \times VR_1} \quad (3)$$

$$GI = \frac{V_{50\%}}{VR_1} \quad (4)$$

where,

$D_{2\%}$ is dose delivered to 2% of the volume, $D_{98\%}$ is dose delivered to 98% of the target volume, TV_1 is target volume covered by the prescribed dose, TV is target volume and VR_1 is total volume of prescribed dose. $V_{50\%}$ represents the volume irradiated by 50% of prescribed dose.

The statistical analysis method used was two-tailed Student's t-test, calculated using TIBCO Statistica version 13.5.0.17 (TIBCO Software Inc). A value of $p < 0.05$ was considered statistically significant.

Results

Phantom measurements

Calculated discrepancies for examined algorithms in water (Eq. 1) were found to be within tolerances proposed for different beam arrangements and levels of complexity [24].

Comparison of calculated and measured absorbed dose at respective points in the semi-anthropomorphic CIRS Thorax phantom for evaluated algorithms is shown in Figures 3 and 4. In Figure 3 differences between measured and calculated absorbed dose for different beam arrangements in the WDE region of the phantom are shown for five measuring points (points 1–5, Fig. 1) and dose calculation algorithms used with respective tolerances [24] .

In Figure 4 differences between measured and calculated absorbed dose in the LDE regions of the phantom are shown for four measuring points (points 6–9, Fig. 1) and dose calculation algorithms used with respective tolerances [24].

In the WDE region of the semi-anthropomorphic phantom (Fig. 3), the mean value of differences for the SS algorithm was 0.05% (from –3.2% to +3.2% with standard deviation SD = 1.23%) and in the LDE region (Fig. 4), it was 0.42% (–1.9% to +3.8%, SD = 1.27%). Considering the good agreement of the measured and calculated data, SS was taken as the algorithm of choice for absorbed dose distribution calculations for radiation therapy of in-situ NSCLC at that time.

Also, absorbed dose calculated using algorithms built in Monaco TPS was compared to measured absorbed dose values. The results in the WDE region

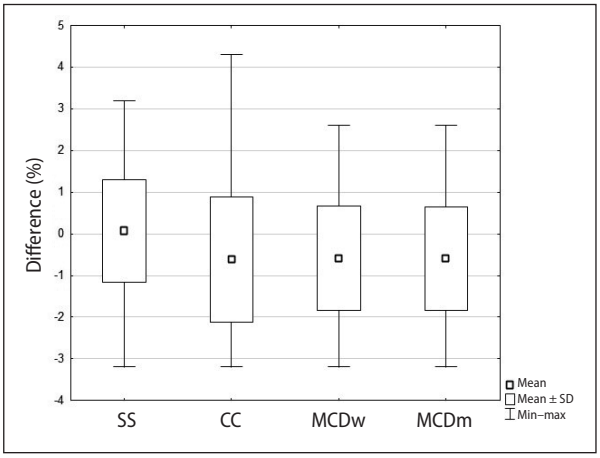

Figure 3. Box and Whisker plot for differences between measured and calculated absorbed dose in WDE region of the semi-anthropomorphic phantom at five measuring points (points 1–5, Fig. 1) for all evaluated algorithms. SS — standard superposition; CC — collapsed cone; MCDm — Monte Carlo dose to medium; MCDw — Monte Carlo recalculation to dose to water from dose to medium

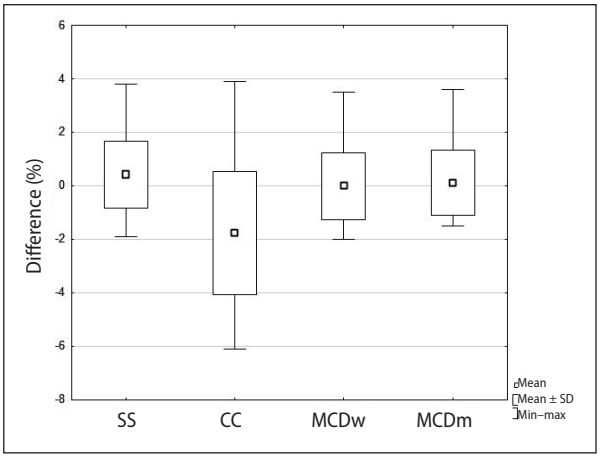

Figure 4. Box and Whisker plot for differences between measured and calculated absorbed dose in lung density equivalent (LDE) regions of the semi-anthropomorphic phantom at four measuring points (6–9, Fig. 1) for all evaluated algorithms. SS — standard superposition; CC — collapsed cone; MCDm — Monte Carlo dose to medium; MCDw — Monte Carlo recalculation to dose to water from dose to medium

(Fig. 3.) are in accordance with the proposed tolerances [24]. For MCD_m calculation, mean difference between the measured and calculated absorbed dose, was –0.59% (from –3.21% up to 2.64%, SD = 1.24%) and for MCD_w mean difference was –0.58% (from –3.24% to 2.58%, SD = 1.25%). The results obtained for the CC algorithm show slightly larger deviations compared to the results of remaining algorithms. The mean difference for CC is –0.62% (from -3.19% to 4.33%, SD = 1.49%) in the WDE region.

In the LDE region (Fig. 4.) of the phantom, the mean differences between the measured and calculated absorbed dose values for all measuring points were: –1.76% (–6.1% to +3.9%, SD = 2.29%) for CC, and 0.12% (–1.5% to +3.6%, SD = 1.21%) for MCD_m, and 0.01% (–2.0% to +3.5%, SD = 1.24%) for MCD_w. These results indicate that for SS, MCD_m and MCD_w differences between calculated values and measurements in the LDE region were in tolerance. Additionally, it should be emphasized that the differences between MCD_m and MCD_w compared with measured absorbed doses for all investigated points in the LDE region are almost the same. On the other hand, more than 20% of results for the CC algorithm were out of tolerance (Fig. 4).

Clinical study

A comparison of absorbed dose distributions calculated using CC, MCD_m and MCD_w versus SS has been carried out for the 15 NSCLC patient data sets. Parameters based on dose calculated using aforementioned algorithms in comparison with SS and corresponding statistical analysis results for NSCLC patients in this study are shown in Tables 1, 2.

TVs and additional structure

Results in Table 1 represent the comparison of CC, MCD_m and MCD_w mean values of examined relevant TV parameters with standard deviations (SD) in relation to SS algorithm values taken as reference. Statistical analysis was performed for GTVs as well as PTVs.

For the GTVs, there is no statistically significant difference neither in prescribed dose coverage (V_{70Gy}) nor in CI, HI and $D_{2\%}$ when CC and MC data are compared with SS. On the other hand, there was a statistically significant difference in D_{mean} between MCD_w and SS (p = 0.020618).

Results of the PTV analysis show different trends. Namely, for the PTVs, there is a statistically significant difference for CC (V_{70Gy}) with the mean value of 86.16% and SD = 3.07% (p = 0.000203), and a statistically significant difference for MCD_m (V_{70Gy}) with the mean value of 96.96% and SD = 1.55% (p = 0.000161), and a statistically significant difference for MCD_w (V_{70Gy}) with the mean value of 96.91% and SD = 1.78% (p = 0.004251) in comparison with the SS mean value of 92.52% and

Table 1. Colapsed cone (CC), Monte Carlo (MC) based algorithm expressed as dose to medium in medium (MCD_m) and dose to water in medium (MCD_w) absorbed dose calculation comparison with standard superposition (SS) for the gross target volume (GTVs) and the planning target volume (PTVs): mean values of relevant parameters with related standard deviations and p-values

Structure	Parameter	SS	CC	CC vs. SS	MCD_m	MCD_m *vs.* SS	MCD_w	MCD_w *vs.* SS
		Mean (SD)	Mean (SD)	p-Value	Mean (SD)	p-value	Mean (SD)	p-value
GTV	V_{70Gy} (%)	99.84 (0.16)	99.67 (0.16)	0.057217	99.86 (0.18)	0.794920	99.72 (0.33)	0.377364
	D_{mean} (Gy)	72.39 (0.35)	72.21 (0.70)	0.535883	72.15 (0.13)	0.088804	72.01 (0.23)	0.020618
	$D_{2\%}$ (Gy)	73.41 (0.13)	73.36 (0.23)	0.621277	73.26 (0.26)	0.168130	73.42 (0.21)	0.891330
	CI	0.27 (0.05)	0.28 (0.06)	0,777953	0.25 (0.07)	0,519527	0.25 (0.07)	0,470062
	HI	1.03 (0.01)	1.04 (0.01)	0.057276	1.03 (0.00)	0.435428	1.03 (0.01)	0.17643
PTV	V_{70Gy} (%)	92.52 (2.17)	86.16 (3.07)	0.000203	96.96(1.55)	0.000161	96.91 (1.78)	0.00425
	D_{mean} (Gy)	71.85 (0.26)	71.51 (0.65)	0.191729	71.75 (0.21)	0.431353	71.68 (0.27)	0.212450
	$D_{2\%}$ [Gy]	73.37 (0.1)	73.38 (0.20)	0.977719	73.34 (0.34)	0.812527	73.39 (0.17)	0.810185
	CI	0.76 (0.05)	0.7 (0.04)	0.024555	0.77 (0.07)	0.855947	0.75 (0.07)	0.751894
	GI	6.19 (1.03)	6.32 (1.09)	0.809451	5.32 (0.67)	0.064004	5.38 (0.61)	0.076091
	HI	1.05 (0.01)	1.07 (0.01)	0.001249	1.04 (0.01)	0.001032	1.04 (0.01)	0.005861

CI — conformity index; GI — gradient index; HI — homogeneity index; p-values in bold are statistically significant

Table 2. Mean values of relevant parameters with related standard deviations for ipsilateral, contralateral and whole lungs for standard superposition (SS), Colapsed cone (CC), Monte Carlo (MC) based algorithm expressed as dose to medium in medium (MCDm) and dose to water in medium (MCDw), with p-values determined by comparison of CC, MCDm, MCDw with SS are shown

Structure	Parameter	CC *vs.*SS		MCDm *vs.* SS		MCDw *vs.* SS	
		Mean diff. (SD)	p-value	Mean diff. (SD)	p-value	Mean diff. (SD)	p-value
Ispilateral lung	V_{5Gy} (%)	0.57 (2.31)	0.94	–0.12 (3.53)	0.99	–0.17 (3.57)	0.98
	V_{20Gy} (%)	–1.39 (1.32)	0.83	–1.99 (2.13)	0.76	–1.68 (2.26)	0.79
	D_{mean} [Gy]	–0.41 (0.64)	0.91	–0.16 (1.38)	0.96	0.01 (1.44)	1.00
Contralateral lung	V_{5Gy} (%)	1.53 (3.03)	0.80	2.41 (4.68)	0.68	1.82 (5.01)	0.76
	V_{20Gy} (%)	–0.16 80.42)	0.85	–0.22 (0.64)	0.78	–0.18 (0.67)	0.83
	D_{mean} [Gy]	0.25 (0.34)	0.74	0.41 (0.63)	0.59	0.4 (0.71)	0.60
Whole lungs	V_{5Gy} (%)	0.53 (2.65)	0.93	0.89 (3.79)	0.88	0.8 (3.72)	0.89
	V_{20Gy} (%)	–0.71 (0.48)	0.83	–0.87 (1.19)	0.80	–0.86 (1.14)	0.80
	D_{mean} [Gy]	–0.04 (0.29)	0.98	0.22 (0.82)	0.91	0.22 (0.8)	0.91

SD — standard deviation

SD = 2.17%. Additionally, for the PTVs, statistically significant differences in CI and HI were observed. The mean CI has a lower value for the CC algorithm of 0.70, SD = 0.04 compared to the SS algorithm mean value of 0.76 and SD = 0.05 (p = 0.024555). The mean HI has a higher value for CC of 1.07, SD=0.10 compared to the SS mean value of 1.05 and SD = 0.01 (p = 0.001249). The mean HI has a lower value for MCD_m (1.04, SD = 0.01, p = 0.001032), and MCD_w (1.04, SD = 0.01, p = 0.005861) compared to the SS mean value.

To further investigate the location of dose differences, an additional structure PTV minus GTV (PTV-GTV) was created and V_{70Gy} was analysed for CC, MCD_m and MCD_w compared to SS calculated absorbed dose distributions.

Analysis of the additional structure (PTV-GTV) revealed that the statistically significant difference was found for average V_{70Gy} coverage for CC (79.34%, SD = 4.42%, p = 0.000363) and for MCD_m and MCD_w (95.42%, SD = 2.24%, p = 0.000075 and 95.06%, SD = 2.98%, p = 0.000372, respectively) compared to SS (88.34%, SD = 3.24%).

OARs

A comparison of absorbed dose distributions was also performed for OARs (ipsilateral, contralateral and whole lungs) where the differences could be expected. The comparison of results for respective OAR is shown in Table 2. For the ipsilateral, contralateral and total lungs no statistically significant differences in D_{mean}, V_{20Gy} and V_{5Gy} were found.

Number of MUs

In addition, the average number of MUs required for the optimization of absorbed dose distributions calculated by different algorithms used in this study has also been analysed.

The results show that there is a statistically significant difference in the number of MUs for MCD_m (average MU = 403, SD = 49 and p = 0.000037) and MCD_w (average MU = 400, SD = 51 and p = 0.000088) compared to SS (average MU = 285, SD = 19). On the other hand, there was no statistically significant difference in the number of MUs for CC (average MU = 298, SD = 10) compared to SS.

Discussion

Comparison of calculated and measured absorbed dose in the LDE region of semi-anthropomorphic phantom showed that discrepancies for the CC algorithm were the most pronounced with about 20% out of tolerance values (Fig. 2). On the other hand, for other algorithms all discrepancies were in tolerance. Findings in this study were in accordance with published data [33, 34] which show discrepancies in the LDE region between absorbed dose values measured and calculated using CC algorithm. Additionally, deviations between measured and MCD_m/MCD_w calculated absorbed doses in the LDE region are in agreement with the results from a previously published study where the deviations between MCD_m/MCD_w calculated

absorbed doses were compared to *ab initio* MC simulation [22].

Further analysis of clinical data related to GTVs has shown statistically significant difference only in D_{mean} when calculated data using MCD_w and SS algorithms are compared ($p = 0.020618$). Despite the statistical significance, D_{mean} averages are above the prescribed dose and the $D_{2\%}$ criteria are fulfilled for both algorithms. This difference, while being statistically significant, is in practice clinically irrelevant because all GTV objectives are fulfilled in both cases. From this perspective, all calculated absorbed dose distributions in this study should be appropriate for clinical use. There is quite a different situation when PTVs were analysed. While mean values of the GI, D_{mean} and $D_{2\%}$ show no statistically significant difference, for V_{70Gy}, CI and HI values statistically significant differences were observed. For mean CI, statistically significant difference for CC compared to the SS algorithm ($p = 0.024555$) implies inferior conformity of absorbed dose distributions calculated using CC compared to SS. The mean HI shows higher value for CC compared to SS ($p = 0.001249$) which implies inferior homogeneity of absorbed dose distributions calculated using CC compared to SS. Additionally, the mean HI has a lower value for MCD_m ($p = 0.001032$) and MCD_w ($p = 0.005861$) compared to SS which implies superior homogeneity of absorbed dose distributions calculated using MCD_m and MCD_w compared to SS.

Observed lower PTV coverage in lung tissue for analytical algorithms compared to the MC based algorithm is in accordance with previously reported findings [35].

An example of difference in V_{70Gy} in DVH comparison of PTVs and GTVs for one patient from the study is shown in Figure 5. Considering the V_{70Gy} for the PTV, lower coverage for CC and higher coverage for the MC algorithm when compared to SS is apparent. For GTV the differences in V_{70Gy} are negligible.

The analysis of additional structure (PTV-GTV) revealed that the average V_{70Gy} coverage decreases more for CC than for SS, when compared with PTV. On the other hand, the results for the MC algorithm imply that its use could be a step forward when compared to SS. Namely, results of the comparisons for the (PTV-GTV) volume confirm that both MCD_m (mean difference = 7.36%, SD = 2.13%) and MCD_w (mean difference = 6.99%, SD = 2.59%)

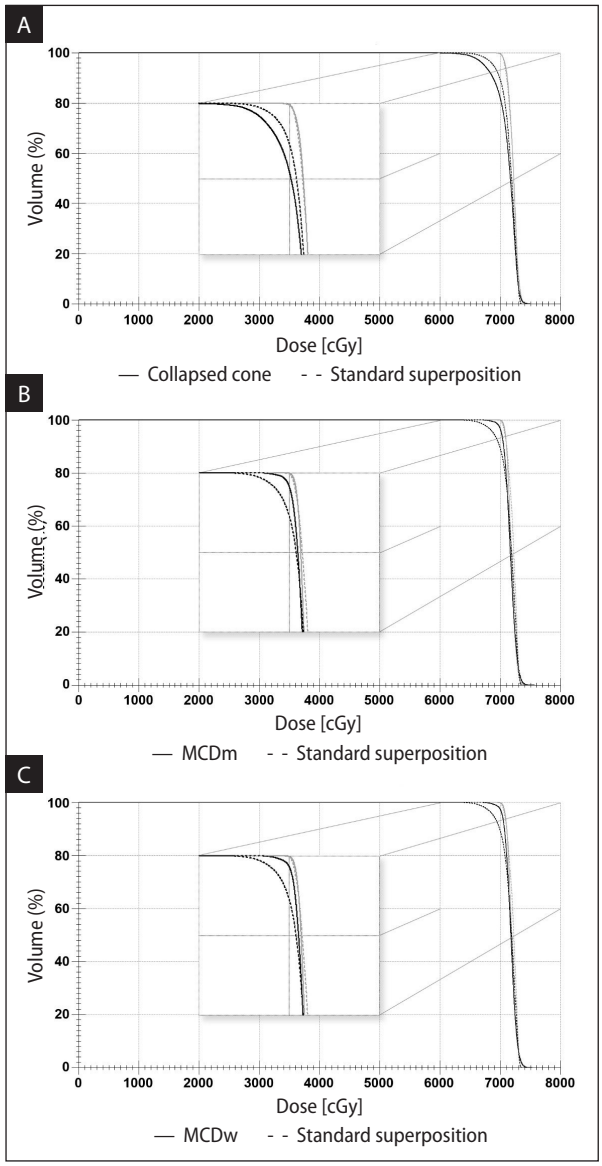

Figure 5. Example of dose volume histograms (DVH) comparison of standard superposition (SS) with collapsed cone (CC) (**A**), Monte Carlo dose to medium (MCDm) (**B**) and Monte Carlo recalculation to dose to water from dose to medium (MCDw) (**C**) for planning target volume (PTV) (black lines) and gross target volume (GTV) (grey lines) coverage for a randomly chosen patient from this study

could provide better coverage than the SS algorithm. A result of a recent study [36] confirms superiority of MC based algorithms in comparison to SS and CC algorithms, especially in GTV coverage. On the other hand, for the CC algorithm, the (PTV-GTV) V_{70Gy} coverage decreases in comparison with absorbed dose distribution calculated by the SS algorithm (mean difference = –8.83%, SD = 3.81%) and also decreases even more than the results for the PTV (Tab. 1). This implies that most

of the differences in calculated dose are located in the low-density part of the PTV considering the high mean coverage of GTV regardless of algorithm used. This result confirms original findings concerning the differences in absorbed dose over the LDE region of the semi-anthropomorphic phantom when measured values and values calculated using the CC algorithm are compared. Statistical analysis was performed for relevant OARs as well (Tab. 2). Considering the large volumes of OARs included in the analysis compared to the volumes of PTVs and GTVs in the chosen group of patients, as well as small differences in CI and GI across the compared absorbed dose distributions, the differences in mean values of analysed parameters in the OARs proved to be negligible and statistically non-significant.

The results related to the average number of MUs required for the optimization of absorbed dose distributions show that there is a statistically significant difference when the number of MUs for MCD_m and MCD_w is compared to SS, which represents a 40% and 41% increase, respectively. This can lead to a substantial increase of treatment duration. On the other hand, there was no statistically significant difference in the number of MUs between investigated analytical algorithms.

Patients with lung cancer have a large probability of inter- and intra-therapy organ and target volume movement due to the respiratory cycle. For that reason, it is necessary to ensure high coverage of target volumes with the prescribed dose and duration of the therapy as short as possible [37]. Additionally, the complexity should be minimized while maintaining all the dose goals for target volumes and organs at risk, especially when intra-therapy image guided radiotherapy (IGRT) and respiratory gating are not available. It is worth noting that in this retrospective study, target volumes and OARs in the thorax are contoured using free breathing CT and empirically determined margins, which introduces a possible substantial geometric uncertainty because the PTV margins are not individualized. For that reason, margins must be large enough to account for such geometric uncertainties. This often results in a larger irradiated volume with higher probability of damage of surrounding healthy tissue, primarily pulmonary. Consequently, lower total prescribed absorbed dose must be applied since lung toxicity is a limiting factor. Considering all the aforementioned, it can be concluded that the use of the CC algorithm for radiotherapy planning of NSCLC cases is inferior to the SS algorithm, which might result in lower quality of overall radiation therapy treatment.

Regarding the results of this study for the MC algorithm in the LDE region, both reporting modes (MCD_m and MCD_w) show equivalent dose volume statistics for relevant TVs and OARs. Additionally, they provide higher prescribed dose coverage for the PTVs than SS or CC.

Additionally, equivalent or superior dose conformity, heterogeneity for TVs and dose parameters for the OARs can be achieved, but at a cost of increased complexity of the treatment and longer radiation therapy time frames.

Conclusion

This work reports the results of a study on the clinical aspects of using different dose calculation algorithms for in-situ NSCLC radiation therapy. The three algorithms built in the Elekta XiO and Monaco treatment planning systems can technically succeed in managing the very restrictive conditions of the clinical goals according to the international standards and are appropriate for treatment planning of NSCLC tumour patients. Nevertheless, this retrospective study shows that the CC algorithm exhibits drawbacks. For this reason, CC users should bear in mind the requirement for higher prescribed dose coverage and higher CI values than the minimal recommendations to achieve adequate treatment quality for NSCLC patients. Namely, lower dose coverage of the target volume and, thus, lower absorbed dose than prescribed, can influence the inferior chances of survival in groups of patients with NSCLC [38, 39]. Additionally, the MC based algorithm used for step and shoot IMRT can fulfil the planning objectives at the expense of higher treatment complexity as well as longer treatment duration, which can also have an impact on therapy quality for NSCLC patients.

Conflict of interest

No conflict of interest.

Funding

This publication was prepared without any external source of funding.

Ethical permission

Ethical approval was not necessary for the preparation of this article.

References

1. Webb S, Nahum AE. A model for calculating tumour control probability in radiotherapy including the effects of inhomogeneous distributions of dose and clonogenic cell density. Phys Med Biol. 1993; 38(6): 653–666, doi: 10.1088/0031-9155/38/6/001, indexed in Pubmed: 8346278.
2. Papanikolaou N, Battista JJ, Boyer AL. AAPM report 85: Tissue Inhomogeneity Corrections for Megavoltage Photon Beams. Report of the AAPM radiation therapy committee task group 65. Medical Physics Publishing, Madison 2004.
3. Fotina I, Winkler P, Künzler T, et al. Advanced kernel methods vs. Monte Carlo-based dose calculation for high energy photon beams. Radiother Oncol. 2009; 93(3): 645–653, doi: 10.1016/j.radonc.2009.10.013, indexed in Pubmed: 19926153.
4. Grofsmid D, Dirkx M, Marijnissen H, et al. Dosimetric validation of a commercial Monte Carlo based IMRT planning system. Med Phys. 2010; 37(2): 540–549, doi: 10.1118/1.3284359, indexed in Pubmed: 20229862.
5. Li J, Galvin J, Harrison A, et al. Dosimetric verification using monte carlo calculations for tissue heterogeneity-corrected conformal treatment plans following RTOG 0813 dosimetric criteria for lung cancer stereotactic body radiotherapy. Int J Radiat Oncol Biol Phys. 2012; 84(2): 508–513, doi: 10.1016/j.ijrobp.2011.12.005, indexed in Pubmed: 22365630.
6. Fotina I, Kragl G, Kroupa B, et al. Clinical comparison of dose calculation using the enhanced collapsed cone algorithm vs. a new Monte Carlo algorithm. Strahlenther Onkol. 2011; 187(7): 433–441, doi: 10.1007/s00066-011-2215-9, indexed in Pubmed: 21713394.
7. Takahashi W, Yamashita H, Saotome N, et al. Evaluation of heterogeneity dose distributions for Stereotactic Radiotherapy (SRT): comparison of commercially available Monte Carlo dose calculation with other algorithms. Radiat Oncol. 2012; 7: 20, doi: 10.1186/1748-717X-7-20, indexed in Pubmed: 22315950.
8. Elcim Y, Dirican B, Yavas O. Dosimetric comparison of pencil beam and Monte Carlo algorithms in conformal lung radiotherapy. J Appl Clin Med Phys. 2018; 19(5): 616–624, doi: 10.1002/acm2.12426, indexed in Pubmed: 30079474.
9. Bosse C, Narayanasamy G, Saenz D, et al. Dose Calculation Comparisons between Three Modern Treatment Planning Systems. J Med Phys. 2020; 45(3): 143–147, doi: 10.4103/jmp.JMP_111_19, indexed in Pubmed: 33487926.
10. Jurković S, Svabić M, Diklić A, et al. Reinforcing of QA/QC programs in radiotherapy departments in Croatia: results of treatment planning system verification. Med Dosim. 2013; 38(1): 100–104, doi: 10.1016/j.meddos.2012.07.008, indexed in Pubmed: 23246197.
11. IAEA Technical report series No. 430: Commissioning and quality assurance of computerized planning system for radiation treatment of cancer. International Atomic Energy Agency, Vienna 2004.
12. Commissioning of radiotherapy treatment planning systems: Testing for typical external beam treatment techniques. International Atomic Energy Agency — TECDOC-1583, Vienna 2008.
13. Giménez-Alventosa V, Antunes PCG, Vijande J, et al. Secondary particle production in tissue-like and shielding materials for light and heavy ions calculated with the Monte-Carlo code SHIELD-HIT. J Radiat Res. 2002; 43 Suppl(10): S93–S97, doi: 10.1269/jrr.43.s93, indexed in Pubmed: 12793738.
14. Radojčić ĐS, Kolacio MŠ, Radojčić M, et al. Comparison of calculated dose distributions reported as dose-to-water and dose-to-medium for intensity-modulated radiotherapy of nasopharyngeal cancer patients. Med Dosim. 2018; 43(4): 363–369, doi: 10.1016/j.meddos.2017.11.008, indexed in Pubmed: 29306538.
15. Wiesmeyer MD. A multigrid approach for accelerating three dimensional photon dose calculation. Med Phys . 1999; 26(1149 (Abstract)).
16. Aarup LR, Nahum AE, Zacharatou C, et al. The effect of different lung densities on the accuracy of various radiotherapy dose calculation methods: implications for tumour coverage. Radiother Oncol. 2009; 91(3): 405–414, doi: 10.1016/j.radonc.2009.01.008, indexed in Pubmed: 19297051.
17. Elekta Monaco Dose Calculation Technical Reference (Crawley, Elekta) (IMPAC Medical Systems Inc. 2013.
18. Fippel M. Fast Monte Carlo dose calculation for photon beams based on the VMC electron algorithm. Med Phys. 1999; 26(8): 1466–1475, doi: 10.1118/1.598676, indexed in Pubmed: 10501045.
19. Walters BRB, Kramer R, Kawrakow I. Dose to medium versus dose to water as an estimator of dose to sensitive skeletal tissue. Phys Med Biol. 2010; 55(16): 4535–4546, doi: 10.1088/0031-9155/55/16/S08, indexed in Pubmed: 20668336.
20. Ma CM, Li J. Dose specification for radiation therapy: dose to water or dose to medium? Phys Med Biol. 2011; 56(10): 3073–3089, doi: 10.1088/0031-9155/56/10/012, indexed in Pubmed: 21508447.
21. Reynaert N, Crop F, Sterpin E, et al. On the conversion of dose to bone to dose to water in radiotherapy treatment planning systems. Phys Imaging Radiat Oncol. 2018; 5: 26–30, doi: 10.1016/j.phro.2018.01.004, indexed in Pubmed: 33458365.
22. Kolacio M, Brkić H, Faj D, et al. Validation of two calculation options built in Elekta Monaco Monte Carlo based algorithm using MCNP code. Radiat Phys Chem. 2021; 179: 109237, doi: 10.1016/j.radphyschem.2020.109237.
23. Netherlands commission of radiation dosimetry. Code of practice for the quality assurance and control for intensity modulated radiotherapy; 2013.
24. Venselaar J, Welleweerd H, Mijnheer B. Tolerances for the accuracy of photon beam dose calculations of treatment planning systems. Radiother Oncol. 2001; 60(2): 191–201, doi: 10.1016/s0167-8140(01)00377-2, indexed in Pubmed: 11439214.
25. Radojcic DS, Casar B, Rajlic D, et al. Experimental validation of Monte Carlo based treatment planning system in bone density equivalent media. Radiol Oncol. 2020; 54(4): 495–504, doi: 10.2478/raon-2020-0051, indexed in Pubmed: 32936784.

26. Bradley JD, Bae K, Graham MV, et al. Primary analysis of the phase II component of a phase I/II dose intensification study using three-dimensional conformal radiation therapy and concurrent chemotherapy for patients with inoperable non-small-cell lung cancer: RTOG 0117. J Clin Oncol. 2010; 28(14): 2475–2480, doi: 10.1200/JCO.2009.27.1205, indexed in Pubmed: 20368547.
27. Marks LB, Yorke ED, Jackson A, et al. Use of normal tissue complication probability models in the clinic. Int J Radiat Oncol Biol Phys. 2010; 76(3 Suppl): S10–S19, doi: 10.1016/j.ijrobp.2009.07.1754, indexed in Pubmed: 20171502.
28. Marks LB, Bentzen SM, Deasy JO, et al. Radiation dose-volume effects in the lung. Int J Radiat Oncol Biol Phys. 2010; 76(3 Suppl): S70–S76, doi: 10.1016/j.ijrobp.2009.06.091, indexed in Pubmed: 20171521.
29. Bentzen SM, Constine LS, Deasy JO, et al. Quantitative Analyses of Normal Tissue Effects in the Clinic (QUANTEC): an introduction to the scientific issues. Int J Radiat Oncol Biol Phys. 2010; 76(3 Suppl): S3–S9, doi: 10.1016/j.ijrobp.2009.09.040, indexed in Pubmed: 20171515.
30. Riet A, Mak A, Moerland M, et al. A conformation number to quantify the degree of conformality in brachytherapy and external beam irradiation: Application to the prostate. Int J Radiat Oncol Biol Phys. 1997; 37(3): 731–736, doi: 10.1016/s0360-3016(96)00601-3, indexed in Pubmed: 9112473.
31. Feuvret L, Noël G, Mazeron JJ, et al. Conformity index: a review. Int J Radiat Oncol Biol Phys. 2006; 64(2): 333–342, doi: 10.1016/j.ijrobp.2005.09.028, indexed in Pubmed: 16414369.
32. Cao T, Dai Z, Ding Z, et al. Analysis of different evaluation indexes for prostate stereotactic body radiation therapy plans: conformity index, homogeneity index and gradient index. Precis Radiat Oncol. 2019; 3(3): 72–79, doi: 10.1002/pro6.1072.
33. Krieger T, Sauer OA. Monte Carlo- versus pencil-beam-/collapsed-cone-dose calculation in a heterogeneous multi-layer phantom. Phys Med Biol. 2005; 50(5): 859–868, doi: 10.1088/0031-9155/50/5/010, indexed in Pubmed: 15798260.
34. Sini C, Broggi S, Fiorino C, et al. Accuracy of dose calculation algorithms for static and rotational IMRT of lung cancer: A phantom study. Phys Med. 2015; 31(4): 382–390, doi: 10.1016/j.ejmp.2015.02.013, indexed in Pubmed: 25801284.
35. Fogliata A, Cozzi L. Dose calculation algorithm accuracy for small fields in non-homogeneous media: The lung SBRT case. Phys Med. 2017; 44: 157–162, doi: 10.1016/j.ejmp.2016.11.104, indexed in Pubmed: 27890568.
36. Lebredonchel S, Lacornerie T, Rault E, et al. About the non-consistency of PTV-based prescription in lung. Phys Med. 2017; 44: 177–187, doi: 10.1016/j.ejmp.2017.03.009, indexed in Pubmed: 28366555.
37. Saito M, Suzuki H, Sano N, et al. Evaluation of the target dose coverage of stereotactic body radiotherapy for lung cancer using helical tomotherapy: A dynamic phantom study. Rep Pract Oncol Radiother. 2020; 25(2): 200–205, doi: 10.1016/j.rpor.2020.01.001, indexed in Pubmed: 32021577.
38. Machtay M, Bae K, Movsas B, et al. Higher biologically effective dose of radiotherapy is associated with improved outcomes for locally advanced non-small cell lung carcinoma treated with chemoradiation: an analysis of the Radiation Therapy Oncology Group. Int J Radiat Oncol Biol Phys. 2012; 82(1): 425–434, doi: 10.1016/j.ijrobp.2010.09.004, indexed in Pubmed: 20980108.
39. Vanderstraeten B, Reynaert N, Paelinck L, et al. Accuracy of patient dose calculation for lung IMRT: A comparison of Monte Carlo, convolution/superposition, and pencil beam computations. Med Phys. 2006; 33(9): 3149–3158, doi: 10.1118/1.2241992, indexed in Pubmed: 17022207.